Comptes Rendus Geoscience
December 2018, Volume 350 Issue 8 Pages 476-486
https://doi.org/10.1016/j.crte.2018.09.003
https://archimer.ifremer.fr/doc/00463/57477/

Paleo-depths reconstruction of the last 550,000 years based on the transfer function on recent and Quaternary benthic foraminifers of the East Corsica margin

Minto'o Charlie Morelle Angue [1, 2, 3, *], Silva Jacinto Ricardo [4], Bassetti Maria-Angela [1, 2], Jouet Gwenael [4]

[1] Univ Perpignan, CEFREM, UMR 5110, Via Domitia,52 Ave Paul Alduy, F-66860 Perpignan, France.
[2] CNRS, CEFREM UMR 5110, 52 Ave Paul Alduy, F-66860 Perpignan, France.
[3] Ecole Normale Super ENS Libreville, Dept Sci Vie & Terre, BP 17009, Libreville, Gabon.
[4] IFREMER, Ctr Bretagne, Lab Envirom Sedimentaires, F-29280 Plouzane, France.

* Corresponding author : Charlie Morelle Angue Minto, email address : mintoocharly@yahoo.fr

Abstract :

In this study, the model H(i) = 109.6103 + C1 × F1(i) + C2 × F2(i) + … + C33 × F33(i) obtained from depth modelling based on 33 recent benthic foraminifer species distribution, has been applied to the fossil benthic foraminifers from the borehole GDEC-4-2 drilled at a water depth of 491 m, in the East-Corsica basin, covering the last 550,000 years. The obtained variations of the paleo-depths show a medium correlation with the oscillations of the relative sea level and also with the fluctuations of the oxygen isotopic ratio (δ18O G. bulloides and δ18O C. pachyderma–C. wuellerstorfi). This newly developed transfer function is accompanied by an error margin of ± 86 m, suggesting that this model will probably be more suitable for a time scale of the order of a million years where sea level variations are recorded with larger amplitudes. Without considering these problems related to amplitudes, it also turns out that the “eustatic” signal of the microfauna is accompanied by a “trophic” signal, which should not to be neglected, especially at a millennial scale time resolution. Thus, the application of this method would require taking into account the bottom trophic effects strongly controlling the distribution of benthic foraminifer assemblages.

Keywords : Benthic foraminifers, East-Corsica basin, Paleo-depths, Transfer function

1. Introduction

Sea level variation reconstruction related to climatic changes are carried out using numerous tools allowing the direct reading of the paleo-levels recorded by the beach rocks, the marine terraces, the coral reefs or by the evaluation of the variations of the ice volumes through the foraminifer oxygen isotopes and submerged speleothem in coastal areas (Bard et al. 1996; Antonioli et al. 2001; Chappell 2002; Cutler et al. 2003; Siddall et al. 2003; Rohling et al. 2009). Those allowed quantifying the amplitudes related to sea level variations.

Qualitative and quantitative methods based on the microfauna assemblage distributions allowing the reconstruction of the paleo-depths are also used to characterize the sea level fluctuations (Hayward 2004; Hohenegger 2005; Morigi et al. 2005; Spezzaferri and Tamburini 2007; Rossi and Horton 2009; Milker et al. 2011). These methods are based on a very good knowledge of the distribution of living foraminifera and on the assumption that the ecological requirements of specific *taxa* have not changed over time. In this study, we use this principle to establish a transfer function in which the recent benthic foraminifer assemblages of the East-Corsican margin are used for modelling the depths according to the formula: $H_{m,j} = a_c, 0 + Z_{j,k}. a_{c,k}$. Where Hm is the modelled depth at sites j. a (c, *) are constants calibrated by correlation from the reference data (i.e. present days assmblages). $Z_{j,k}$ is a matrix providing at each modelled site j and associated to the assemblage value of the principal component k.

The level of correlation observed between these modeled depths and the actual depths will allow the application of this equation to fossil benthic foraminifer assemblages. Comparison with other eustatic curves will allow discussing this method of sea level reconstruction and evaluating the difficulties of using benthic assemblages as tools of variations in the water column.

2. Study area

Located in the northern part of the Tyrrhenian Sea (Western Mediterranean), the East-Corsica margin, is a continental shelf region varying from 5 to 10 km in width in the northern part to 25 km in the south. The continental shelf characterizing the East-Corsica margin is narrow with a shelf break situated around 110–120 m (Gervais, 2002 ; Gervais et al., 2004). This continental shelf is followed by a steep continental slope incised by numerous meandering canyons (Gervais, 2002). The latter open out into a deep basin, which is characterized by a depression named Corsican Trough.

3. Materials and methods

3.1. Micropaleontological and stable isotope analyses

Before performing micropaleontological analyses, samples were washed and sieved (63 µm) on the sedimentary fraction > 150 µm. The recent benthic foraminifers of the East-Corsica basin were studied in 45 surface samples from the interface cores collected at depths ranging from 7 to 868 m and 101 benthic foraminifer *taxa* were identified (Angue Minto'o et al., 2013). The identification of 84 *taxa* of fossil benthic foraminifer was possible via the analysis of 291 samples from GDEC-4 borehole drilled at a water depth of 492 m in the East-Corsica margin covering the last 550,000 years (Angue Minto'o et al., 2016).

Oxygen stable isotope measurements were performed on specimens of planktonic foraminifera species *Globigerina bulloides* and *G. ruber* (white) from the 250–315 µm size fraction, *Neogloboquadrina pachyderm*a (dextral) from the 200–250 µm size fraction, and on the epifaunal benthic foraminifera *Cibicides wuellerstorfi, Cibicidoides pachyderma* and *Cibicidoides kullenbergi* found in the > 150 µm size fraction (Toucanne et al., 2015).

3.2. Species selection and Principal component analysis

In this study MatLab generic functions is used for the computations. We call M_0 (i,j), the initial matrix of species to be consider in the analysis. M_0 (i,j) consists of relative abundances of the all benthic foraminifers (101 species) identified in the surface samples: where i is the sites and j the species. In aim to have qualitative results, the reduction of number of species of M_0 (i,j*)* is made by eliminating species with a median equal 0. Because the Principal Component Analysis (PCA) is based on correlation analysis and hence variation quantifications. Consequently, on 101 recent benthic foraminifer taxa identified, only 33 taxa

were retained and are listed in the table 1. For these 33 species, the relative abundance, at one site, is always calculated on the total number of individuals per site based on the 101 species. This allowed maintaining independence between the frequencies retained, i.e. the sum of the species frequencies per site does not equal 1, and the dependent and untreated variable is «the other species» :

$\sum_{j=1}^{33} M_{ij} \leq 1$ where M is the abundance matrix of site **i** and of species j. The analysis is based on the abundance matrix M expressing at each site I (from 1 to ***) the abundance of each species j (from 1 to 33). Each value of M is hence expressed by M_{ij}.

PCA is based on the covariance matrix (M_c) estimated on the basis of the species abundance matrix by site:

$M_{c, kj} = \text{cov}\ (M_{ij}, M_{ik})$

$M_{c, kj}$ represents the correlation between species k and j for the all sites i. $M_{c, kj} = M_{c, jk}$.

The eigenvalues and eigenvectors of the matrix Mc are computed to establish, respectively, the weight (variance) associated with each component and the coefficients of the principal components. Thus, the matrix of the eigenvectors C_{jk}, and coefficients of the principal components, is calculated as well as the diagonal matrix of the eigenvalues D_{jk}. The new matrix C_{jk} checks the following equality:

$M_{c, kj}. C_{jk} = C_{jk} . D_{jk}$

The principal components are obtained by a "rotation" of the assembly matrix (M_{ij}) along the principal vectors described by the matrix of eigenvectors or coefficients of the components

$Z_{ik} = M_{ij} . C_{jk}$

It is important to remenber that matrix Z_{ik} contains the same amount of information than the initial abundance matrix Mij from which Z_{ik} has been derived. The information is organised in a new way, the components being independent one from the others. Hence, at each site i the

Z_{ik} provides the local value of component k, while M_{ij} provides the local abundance of specie j. The number of species and of components being the same (33).

The matrix C_{jk} co-relates the principal components and the species. Even if it is computed from the data it contains an estimation of a relation that is supposed to be valid to any assemblages (not just the ones in the data). C_{jk} is the same to all sites (observed or note) and is the base of the generalization.

At each new site :

$H_k = a.Z_k + b = a \, . \, C_{kj} \, . \, M_j + b$

We can evaluate the possibility to obtain a model linking the species assemblages and the depth of the sites by the correlation levels with depth of the different components, on the one hand, and the linear combinations of components, on the other hand.

3.3. One-Component Models

For each component Z_k, one can define a depth model H_k obtained by linear regression for depth H:

$H_k = a.Z_k + b$

Where the coefficients a and b are estimated by the least squares method for each component. Thus a function B_k can be defined. This function gives the correlation level (coefficient) obtained by regression (R) between the modeled depth H_k and the true depth H.

$B_k = R (H_k, H)$

3.4. Multi-component models

For models consisting of several components the method applied is the same. A depth model is obtained by linear regression using the least squares method. Here the most representative component of the variance is used. Thus, a depth model H_n can be defined, where n is the number of components used (from the highest to the lowest):

$$H_n = a_0 + \sum_{k=1}^{n} a_{ij}.Z_k$$

The performance of the model H_n can be associated with the A_n function

$$A_n = R\ (H_n, H)$$

The value A_6 will give the correlation level of a regression model based on the 6 most important components in terms of assemblage variability.

3.5. Determination of the freedom factor

A freedom factor (λ_n) of a model consisting of principal components n with respect to the points number (P) of calibration / validation is defined by the following formula

$$\lambda_n = \frac{P-(n+1)}{P}$$

A freedom factor is defined to quantify the robustness of the models based on the number of its number of freedom degrees. For a model based on n principal components, its freedom factor (L_n) is quantified by the number of data points used for calibration (P) and the number of degrees of freedom of the used model (n+1, if n PC are used).

If this factor is close to the unit, the model is robust in terms of degrees of freedom. If the factor is close to zero, the model is not robust and and there are too many degrees of freedom compared to the size of the data available and the basis of its construction. In our study P = 44.

An indicator of performance of model could be defined as the "good" compromise between the correlation level and its performance or factor of freedom. The quality of a model H_n described by the function Qn is defined as follows:

$$Q_n = R(H_n, H) \cdot \lambda_n = A_n \cdot \lambda_n$$

3.6. Calibration and validation of models

After a ranking based on their depths, the 44 sites are divided into two groups. The first group is composed of one site out of two and it is called “calibration”. This group includes variables with an index "c". The second group consists of the other sites and it is called “validation”. This validation group is characterized by variables with an index "v". The coefficients a_k are calculated by regression on the basis of the following system of equations:

$$a_0 + Z_{ik} \cdot a_k = H_i$$

The modeled values will then be:

$$H_{m,i} = a_0 + Z_{i,k} \cdot a_k$$

Where a_k represents the regression coefficients estimated by the least squares method and Z_{ik} represents the principal component value k at site i. H_i is the true depth at site i and H_m, i represents the depth modeled at point i. As we have 22 sites for calibration and validation, it is clear that the number of components must be well below this number (we tested from 1 to 6 components). The real model is based on calibration data (i.e. sites). The associated coefficients are thus obtained:

$$a_{c,0} + Z_{c,k} \cdot a_{c,k} = H_c$$

The calibration coefficients are then used for the validation data in order to obtain the simulated data $H_{m,v}$

$$H_{m,j} = a_{c,0} + Z_{jk} \cdot a_{c,k}.$$

4. Results and discussion

4.1. Principal Component Analysis (PCA)

The results of the PCA show that a very important part of the variance (> 90%) is contained in the first 5 eigenvalues, or principal components (Fig. 1). The contribution of each

species to the two main components can be visualized by the respective contributions of each species (Fig. 2). It may be noted in figure 2 that the species that contribute the most to the expression of the first component are *M. barleeanus* (21) and *U. mediterranea* (33). This component is modulated (attenuated) by the presence of *C. carinata* (11), *R. globularis* (26) and *Q. duthiersi* (23). The second component, however, is expressed by the "competition" between *C. carinata* and *R. globularis* (Fig. 2).

4.2. Correlation between depths and principal components

The correlation levels between the depth of the sites and the principal components associated with the assemblages are presented in the figure 3. Function B is represented by the blue bars that indicate the correlation level of each component with the depth. The function A is represented by the red curve. This latter indicates the correlation level reached by regression between a set of N components and the depth. Thus, the component 33 which is the first in importance is the one that shows the best correlation with the depth. This component alone allows having a correlation level higher than 95% (Fig. 3). The other components are individually weaker. However, they allow increasing the total correlation to more than 99% if all 33 components are used to reproduce the 44 depths.

The best model is not necessarily the one that allows obtaining the best correlation between true values and model values estimated on these same true values. The number of degrees of freedom associated with the calibrated models and the number of validation points must be taken into account, because the models are calibrated on the validation points. Thus, all models H_k have two degrees of freedom: the coefficients a and b. The models H_n, have n + 1 degrees of freedom. By absurdity, a model whose number of degrees of freedom is equal to the number of calibration / validation points will always presented a correlation of 100%. Because the data is taken as their own model; the practical value of such model is null.

The representation of the function Q_n (Fig. 4) shows that the use of a small number of components can be advantageous in terms of the robustness of the chosen model.

4.3. Evaluation of models

The evaluation is made for models built with a number of variable components (between 1 and 6). The model with all the data (blue curve) serves as a reference (Fig. 5). Calibration 1 (Cal 1) and Validation 1 (Val 1) are obtained as described in the calibration and validation of models paragraph: The first set is for calibration and the second set for validation. The models cal. 2 and val. 2 are obtained by reversing the use of sets (Fig. 5).

For cal. and val. 1, we obtain a calibration model that is slightly less efficient than the reference model. While, the validation is generally better (Fig. 5). This means that the validation set is closer, in terms of assemblages, to what can be explained by the depth. Overall, the correlation improves with the number of components used. This improvement is increasing for reference and for the calibration (Fig. 5). For the validation model, the two minor contribution components (2 and 5) reduce the performance of the model. When we reverse the use of sets, we fall back on a reverse result, and more «classic». Calibration, done on less data than the reference, is more efficient (but with a lower freedom factor); validation is less well than calibration and reference.

The choice seems to be made between 1, 4 or 6 components. Even if it remains conceivable to use only the useful components. Correlations are performance indicators. It is therefore important to visualize the correlations presented in Figures 6 and 7 in which a loss of linearity can be observed from 700 m depth with the error margins of 43 m and thus 86 m in 2σ.

4.4. Choice of the final model

Principal component analysis allows us to « focus» the variance of the assemblages on a very small number of variables (components), which is very useful in order to reduce the number of freedom degrees of the models obtained by regression.

Out of 33 components (as much as the selected species), we will keep 4 components (28, 30, 31 and 33). Which means that the regression model is based on the estimation of 5 parameters.

The model obtained made it possible to have a 97.13% correlation on all the sites. The calibrated model on 22 sites (performance of 96.85% in self-application) displays a correlation of 97.72% on the validation set. The performance of the chosen model is illustrated in the figure 8.

4.5. The structure of the model

The structure of the model is presented in figure 9. It can be noted that the final contribution to explaining depth variability is very distinct from the distribution of the coefficients associated with each species. This is because the relative abundance of each species has not been standardized. Thus, there are two species that contribute significantly: *M. barleeanus* and *U. mediterranea*. *M. barleeanus* explains the variations of depth at shallow depth and *U. mediterranea* explains the depth beyond 100 m depth.

4.6. Application of the model and comparison with the semi-quantitative method

4.6.1 Numerical model

The application of the model H (i) = 109.6103 + C1 * F1 (i) + C2 * F2 (i) + ... + C33 * F33 (i) (where Ci corresponds to the coefficient of species i and Fi to its frequency) on fossil

benthic foraminifers species allowed to obtain the curve of paleo-depths variation. The reconstructed palaeo-depths range from 622 ± 86 m to 21 ± 86 m. In general, the variation of these paleo-depths correlates quite well with the variations of the sea level (Fig.10). A global trend marked by an increase in depth during periods of high sea level is observed. Interglacials are characterized by the removal (or melting) of glaciers that conduct to an increase in sea level (Dorale et al. 2010) and therefore an increase in the water level above the seabed. This could justify this rise of the paleo-depths during these warm climatic periods. However, these paleo-depth variations are characterized by very large amplitudes.

Based on the fact that these modeled amplitudes are affected by: 1 / local effects related to the morphology of the basin which is shallow and semi-marine (close to the sources); 2 / changes in trophic conditions at the bottom strongly influencing the variations of benthic microfauna assemblages; 3 / uncertainties related to the calculation method and the bathymetry. Normalization from 0 to 120 m was thus made on the values of paleo-depths and the sea level variation curve obtained was compared with the eustatic curve established by Rohling et al. (2009) and smoothed in the same way (Fig. 11). This results in a fairly good correlation between these two curves.

However, very large temporal offsets in amplitude and in time are observed between the two interglacial curves: between 290 and 280,000 years (15 ka), 200 and 180,000 years (15 ka), 170 and 160,000 years (15 ka), 125 and 100,000 years (30 ka) and between 60 and 30,000 years (30 ka, Fig. 11).

These offsets therefore appear during periods of high sea level that are globally characterized by a decrease in the organic matter inputs related to the theoretical distance of the sources (Cortina et al., 2013) and by a decrease in the ventilation at the sea bottom (Toucanne et al., 2012). The offsets result from an underestimation of the depths that could be related to the non-integration, in the model, of the changes in bottom trophic conditions strongly influencing the variations of benthos foraminifer assemblages (Mackensen et al. 1990; Murray

1991; Jorissen et al. 1995; De Rijk et al. 2000; Fontanier et al. 2002; Schönfeld 2002a; Schönfeld 2002b; Gooday 2003). Indeed, *U. mediterranea* and *M. barleeanus* are the two species of benthic foraminifers that strongly influence the calculation of paleo-depth. This is illustrated by the perfect correlation between the normalized eustatic variation curve and the variation in their cumulative abundance curve (Fig. 11). *U. mediterranea and M. barleeanus* are species related not only to the quality but also to the intensity of organic matter inputs to the bottom. *M. barleeanus* is known as a species that develops in environments where there is the refractory organic matter (Lutze and Coulbourn, 1984 ; Fontanier et al., 2002) and *U. mediterranea* adapts to environments with moderate fluxes of labile organic matter (Lutze and Coulbourn, 1984 ; Schmiedl et al., 2000).

Based on this low correlation and the error margins obtained (± 86 m), and on the significant offsets observed with the relative sea level variation curve (15 and 30 ka), we can say that on a time scale 100,000 years, the method is difficult to apply. Because at this time scale, the variation amplitudes of the sea level (the order of one hundred meters), remain lower compared to the margin of error (± 86 m) applied to our model. The transfer function could therefore be more suitable on a millions years time scale in which sea level variations are recorded with larger amplitudes and where isotopes are difficult to use.

5. Conclusion

Depth modeling using 33 species of recent benthic foraminifers in the East Corsica margin was based on a principal component analysis (PCA) that allow to obtain the model H (i) = 109.6103 + C1 * F1 (i) + C2 * F2 (i) + ... + C33 * F33 (i) with a correlation of 97.1%. The application of this model on fossil benthic foraminifers conducts to the establishment of a paleo-depth variation curve with a margin of error of ± 86 m. The resulting sea-level variation curve shows significant shifts during high sea levels, which could partly be explained by the significant evolution of trophic conditions during interglacial periods. This margin of error and

this offset can be indicators of the limit of application of this transfer function on a scale of 100,000 years where the sea level variation amplitudes are the order of a hundred meters. On the other hand, on a million-year scale that is characterized by variation with larger amplitudes, this model could provide an interesting estimation. In order to reduce the margin of error and to avoid a significant signal disturbance it is necessary to taking into account in the function of transfer, the environmental parameters, in particular the concentration and quality of the organic matter and other nutrients that largely affect the bathymetric distribution of benthic foraminifers.

References

Angue Minto'o, C.M., Bassetti M.A., Jouet, G., Toucanne, S., 2013. Distribution of modern ostracods and benthic foraminifers from the Golo margin (East-Corsica). In Colin, J.-P. & J. Sauvagnat (Eds), 27e Réunion des Ostracodologistes de Langue Française (ROLF) en l'honneur de H.J. Oertli, 1-3 juin 2012iddal, Revue de Paléobiologie, 32 (2): 607-628.

Angue Minto'o, C.M., Bassetti M.-A., S. Toucanne, G. Jouet, 2016. Distribution of ostracod and benthic foraminiferal assemblages during the last 550 kyr in the East-Corsica basin, western Mediterranean Sea: A paleo-environmental reconstruction. Revue de Micropaléontologie.

Antonioli, F., Silenzi, S., Frisia, S., 2001. Tyrrhenian Holocene palaeoclimate trends from spelean serpulids. Quaternary Science Reviews 20, 1661-1670.

Bard, E., Hamelin, B., Arnold, M., Montaggioni, L., Cabioch, G., Faure, G., Rougerie, F., 1996. Deglacial sea-level record from Tahiti corals and the timing of global meltwater discharge. Nature 382, 241-244.

Chappell, J. (2002). "Sea level changes forced ice breakouts in the Last Glacial cycle: new results from coral terraces." Quaternary Science Reviews 21: 1229-1240.

Cortina, A., Sierro, F.J., Filippelli, G., Flores, J.A., Berné, S., 2013. Changes in planktic and benthic foraminifer assemblages in the Gulf of Lions, off south France: Response to climate and sea level change from MIS 6 to MIS 11. Geochemistry, Geophysics, Geosystems 14, 1258-1276.

Cutler, K.B., Edwards, R.L., Taylor, F.W., Cheng, H., Adkins, J., Gallup, C.D., Cutler, P.M., Burr, G.S., Bloom, A.L., 2003. Rapid sea-level fall and deep-ocean temperature change since the last interglacial period. Earth and Planetary Science Letters 206, 253-271.

De Rijk, S., Jorissen, F.J., Rohling, E.J., Troelstra, S.R., 2000. Organic flux control on bathymetric zonation of Mediterranean benthic foraminifera. Marine Micropaleontology 40, 151-166.

Dorale, J.A., Onac, B.P., Fornós, J.J., Ginés, J., Ginés, A., Tuccimei, P., Peate, D.W., 2010. Sea-Level Highstand 81,000 Years Ago in Mallorca. Science 327, 860-863.

Fontanier, C., Jorissen, F.J., Licari, L., Alexandre, A., Anschutz, P., Carbonel, P., 2002. Live benthic foraminiferal faunas from the Bay of Biscay: faunal density, composition, and microhabitats. Deep Sea Research Part I: Oceanographic Research Papers 49, 751-785.

Gervais, A., 2002. Analyse multi-échelles de la morphologie, de la géométrieet de l'architecture d'un système turbiditique sableux profond (système duGolo, marge est-Corse, Mer méditerranée), 1. Université Bordeaux, pp. 315.

Gervais, A., Savoye, B., Mulder, T., Piper, D.J.W., Cremer, M., Pichevin, L.,2004. Present morphology and depositional architecture of a sandy sub-marine system: the Golo turbidite system (Eastern margin of Corsica). In:Joseph, P., Lomas, S.A. (Eds.), Confined turbidite systems. Geological Soci-ety, London, pp. 59–89.

Gooday, A. J. (2003). Benthic foraminifera (Protista) as tools in deep-water palaeoceanography: environmental influences on faunal characteristics. Advances in Marine Biology. A. J. Southward, P. A. Tyler, C. M. Young and L. A. Fuiman. London, Academic Press. 46: 3-90.

Hayward, B. W. (2004). "Foraminifera-based estimates of paleobathymetry using Modern Analogue Technique, and the subsidence history of the early Miocene Waitemata Basin." New Zealand Journal of Geology and Geophysics 47: 749-767.

Hohenegger, J. (2005). "Estimation of environmental paleogradient values based on presence/absence data: a case study using benthic foraminifera for paleodepth estimation." Palaeogeography, Palaeoclimatology, Palaeoecology 217: 115–130.

Jorissen, F.J., de Stigter, H.C., Vidmark, J.V., 1995. A conceptual model explaining benthic foraminiferal microhabitats. Marine Micropaleontology 26, 3-15.

Lutze, G.F., Coulbourn, W.T., 1984. Recent benthic foraminifera from the continental margin of northwest Africa: Community structure and distribution. Marine Micropaleontology 8 (5), 361-401.

Mackensen, A., Grobe, H., Kuhn, G., Fütterer, D., 1990. Benthic foraminiferal assemblages from the eastern Weddell Sea between 68 and 73°S: Distribution, ecology and fossilization potential. Marine Micropaleontology 16, 241-283.

Milker, Y., Schmiedl, G., Betzler, C., 2011. Paleobathymetric history of the Western Mediterranean Sea shelf during the latest glacial period and the Holocene: Quantitative reconstructions based on foraminiferal transfer functions. Palaeogeography, Palaeoclimatology, Palaeoecology 307, 324-338.

Morigi, C., Jorissen, F.J., Fraticelli, S., Horton, B.P., Principi, M., Sabbatini, A., Capotondi, L., Curzi, P.V., Negri, A., 2005. Benthic foraminiferal evidence for the formation of the Holocene mud-belt and bathymetrical evolution in the central Adriatic Sea. Marine Micropaleontology 57, 25-49.

Murray, J. W. (1991). Ecology and Palaeoecology of Benthic Foraminifera. Longman, Scientific and Tachnical, London, 397 pp.

Rohling, E.J., Grant, K., Bolshaw, M., Roberts, A.P., Siddall, M., Hemleben, C., Kucera, M., 2009. Antarctic temperature and global sea level closely coupled over the past five glacial cycles. Nature Geosci advanced online publication.

Rossi, V. and B. P. Horton (2009). "The application of subtidal foraminifera-based transfer function to reconstruct Holocene paleobathymetry of the Po Delta, northern Adriatic Sea." Journal of Foraminiferal Research 39(3): 180–190.
Schmiedl, G., de Bovée, F., Buscail, R., Charrière, B., Hemleben, C., Medernach, L., Picon, P., 2000. Trophic control of benthic foraminiferal abundance and microhabitat in the bathyal Gulf of Lions, western Mediterranean Sea. Marine Micropaleontology 40, 167-188.
Schönfeld, J. (2002a). "Recent benthic foraminiferal assemblages in deep high-energy environments from the Gulf of Cadiz (Spain)." Marine Micropaleontology 44(3–4): 141-162.
Schönfeld, J. (2002b). "A new benthic foraminiferal proxy for near-bottom current velocities in the Gulf of Cadiz, northeastern Atlantic Ocean." Deep Sea Research Part I: Oceanographic Research Papers 49(10): 1853-1875.
Siddall, M., Rohling, E.J., Almogi-Labin, A., Hemleben, C., Meischner, D., Schmelzer, I., Smeed, D.A., 2003. Sea-level fluctuations during the last glacial cycle. Nature 423, 853-858.

Spezzaferri, S. and F. Tamburini (2007). "Paleodepth variations on the Eratosthenes Seamount (Eastern Mediterranean): sea-level changes or subsidence?" eEarth Discussions 2: 115–132.
Toucanne, S., Jouet, G., Ducassou, E., Bassetti, M.A., Dennielou, B., Angue Minto'o, C.M., Touyet, N., Charlier, K., Lericolais, G., Mulder, T., 2012. A 130,000-year record of Levantine Intermediate Water flow variability in the Corsica Trough, Western Mediterranean Sea. *Quaternary Science Reviews*, Vol. 33, P. 55-73.
Toucanne, S., Angue Minto'o, C.M., Fontanier, C., Bassetti M.-A., Jorry, S.J., G. Jouet, 2015. Tracking rainfall in the northern Mediterranean borderlands during sapropel deposition. *Quaternary Science Reviews*, Vol. 129, P. 178-195.

Figures captions

Figure 1: Variance associated with the 33 main components. The majority of the variance is contained in the first 5 eigenvalues, or principal components.

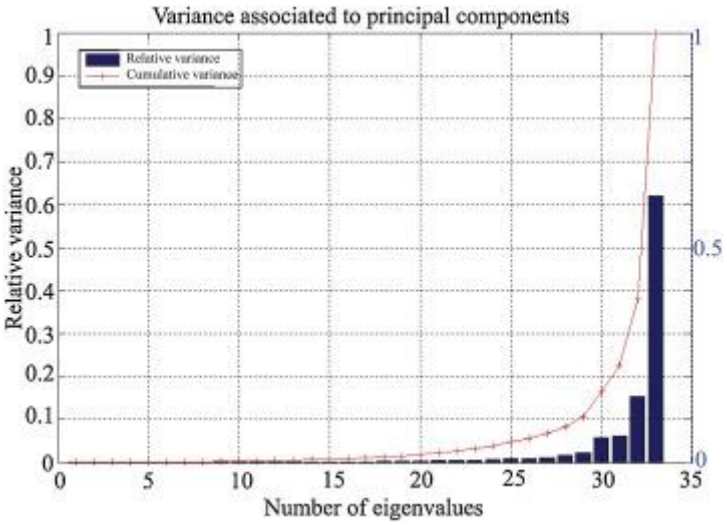

Figure 2: Species contribution to the two main components.

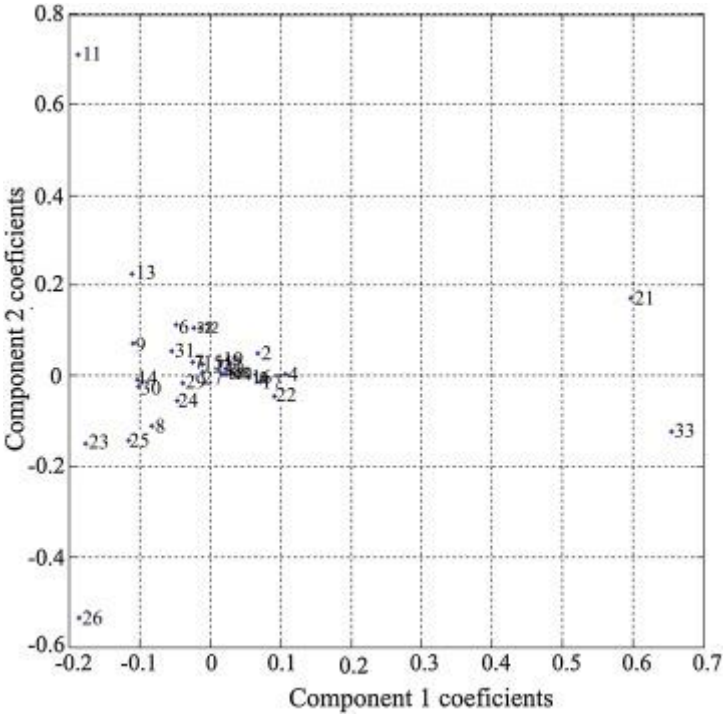

Figure 3: Correlation between depth of the sites and the principal components. The blue bars represent the function B and the red curve characterizes the function A.

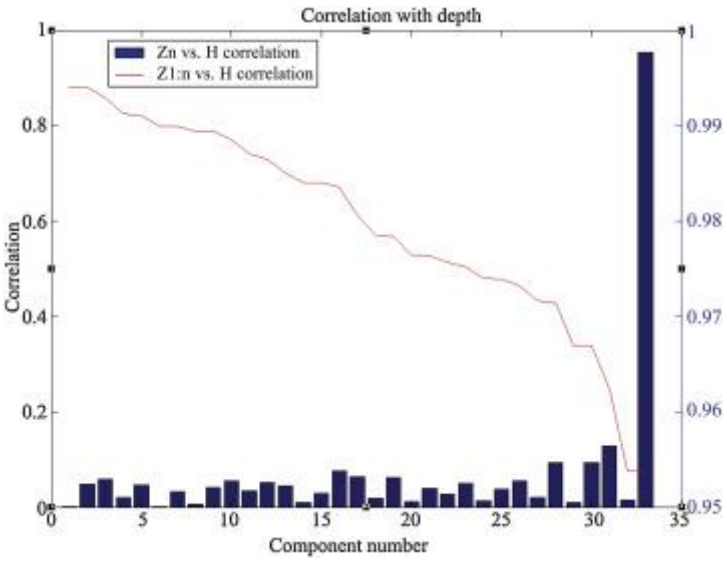

Figure 4: Representation of the fonction Qn.

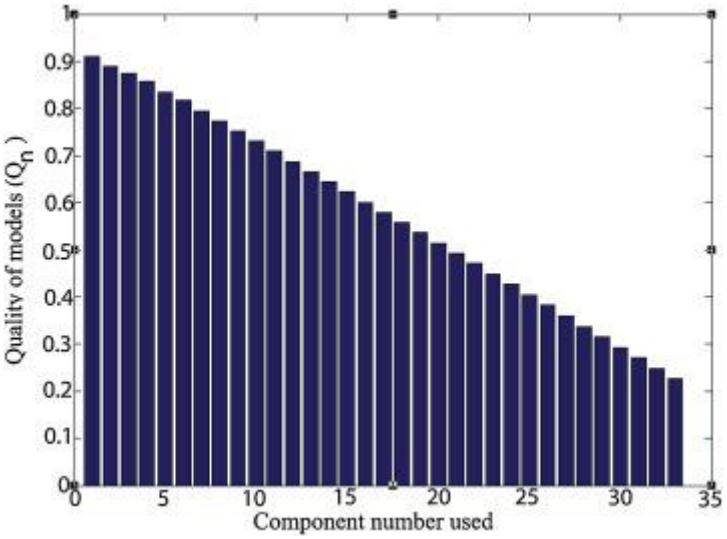

Figure 5: Evaluation of the different models: the one with all the data (blue curve) and the models calibration (green curves) and validation (orange curves).

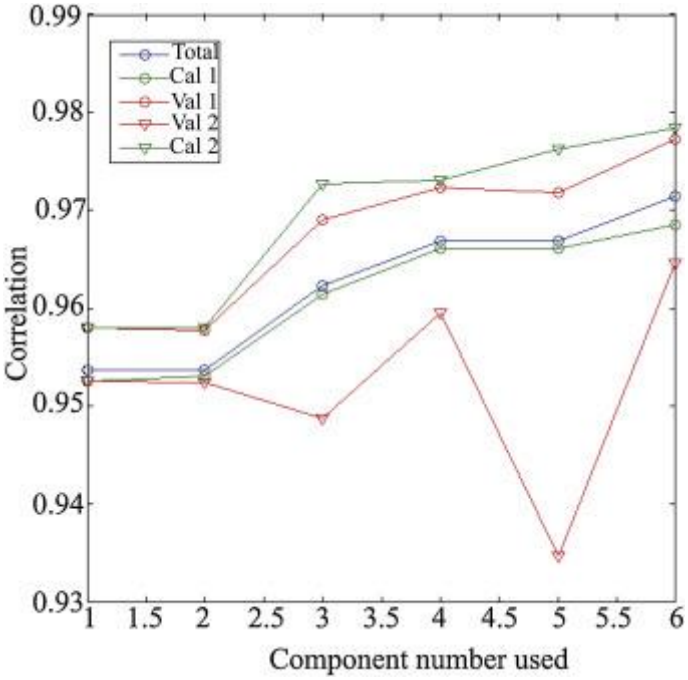

Figure 6: Correlation for models with the use of 1 to 6 main components (from top left to bottom right). Calibration set: cal. 1. Reference (blue), calibration (green) and validation (red).

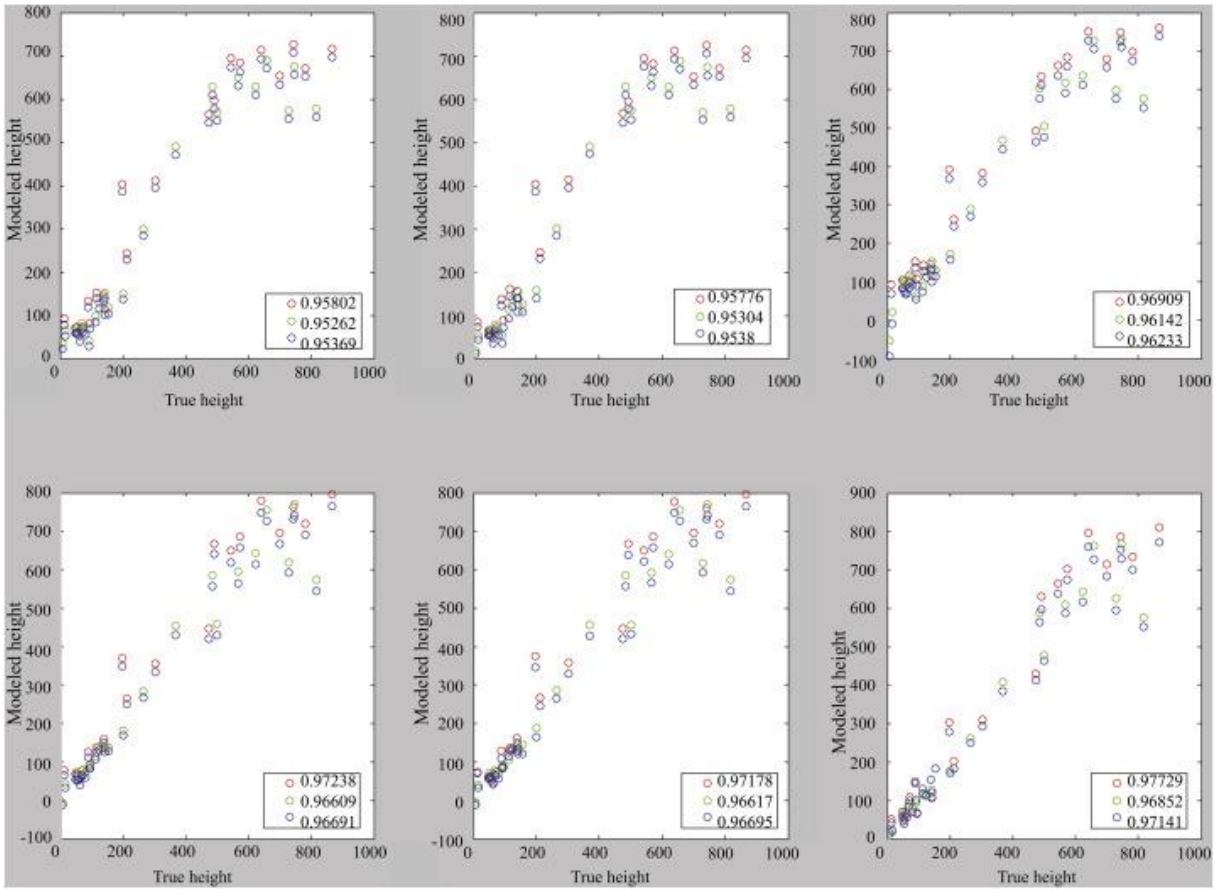

Figure 7: Correlation for models with the use of 1 to 6 main components (from top left to bottom right). Calibration set: cal. 2. Reference (blue), calibration (green) and validation (red).

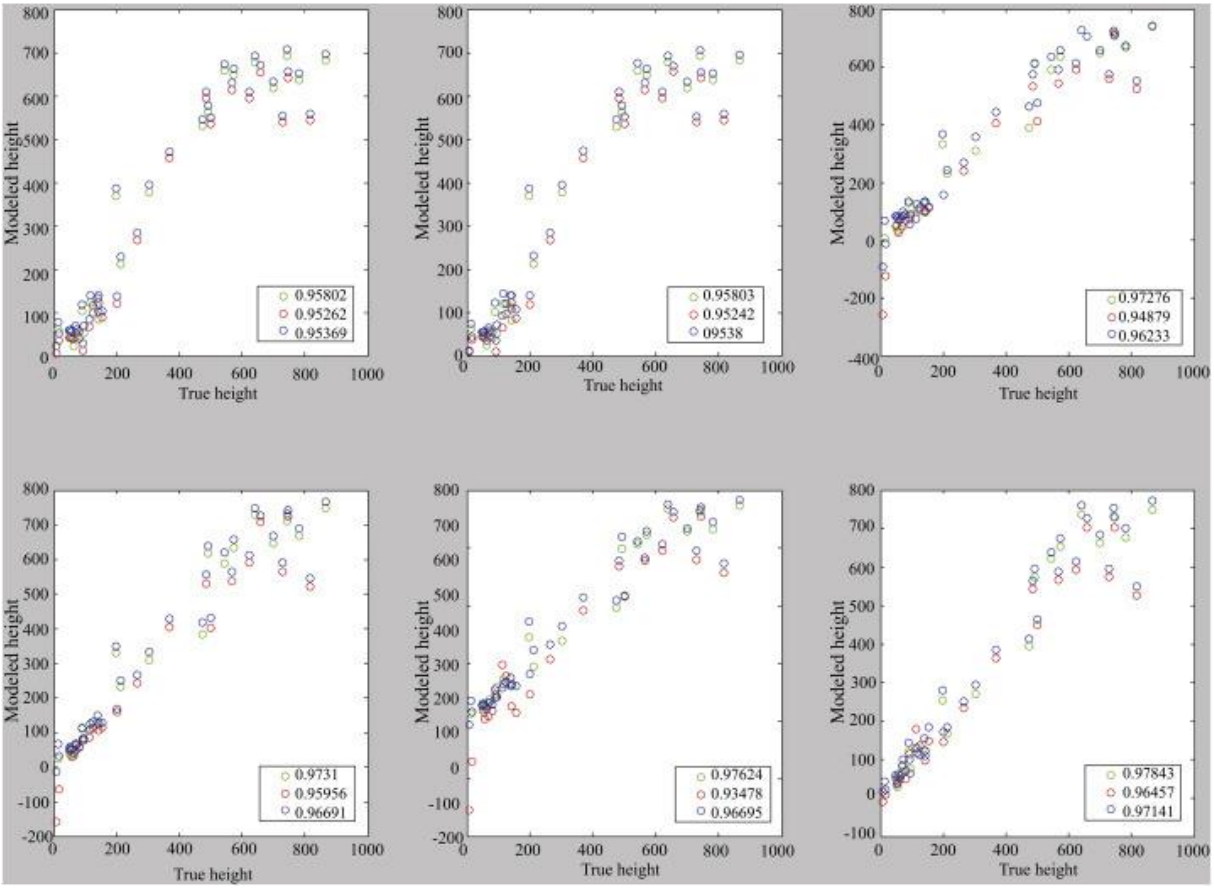

Figure 8: Performance of the selected model: correlation between "true" depths and modeled depths.

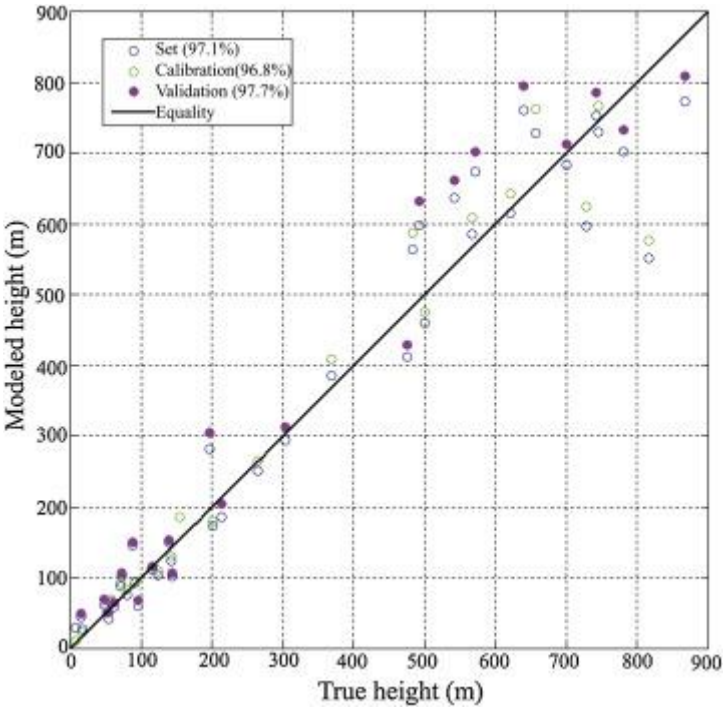

Figure 9: Model structure: coefficients and variance by species.

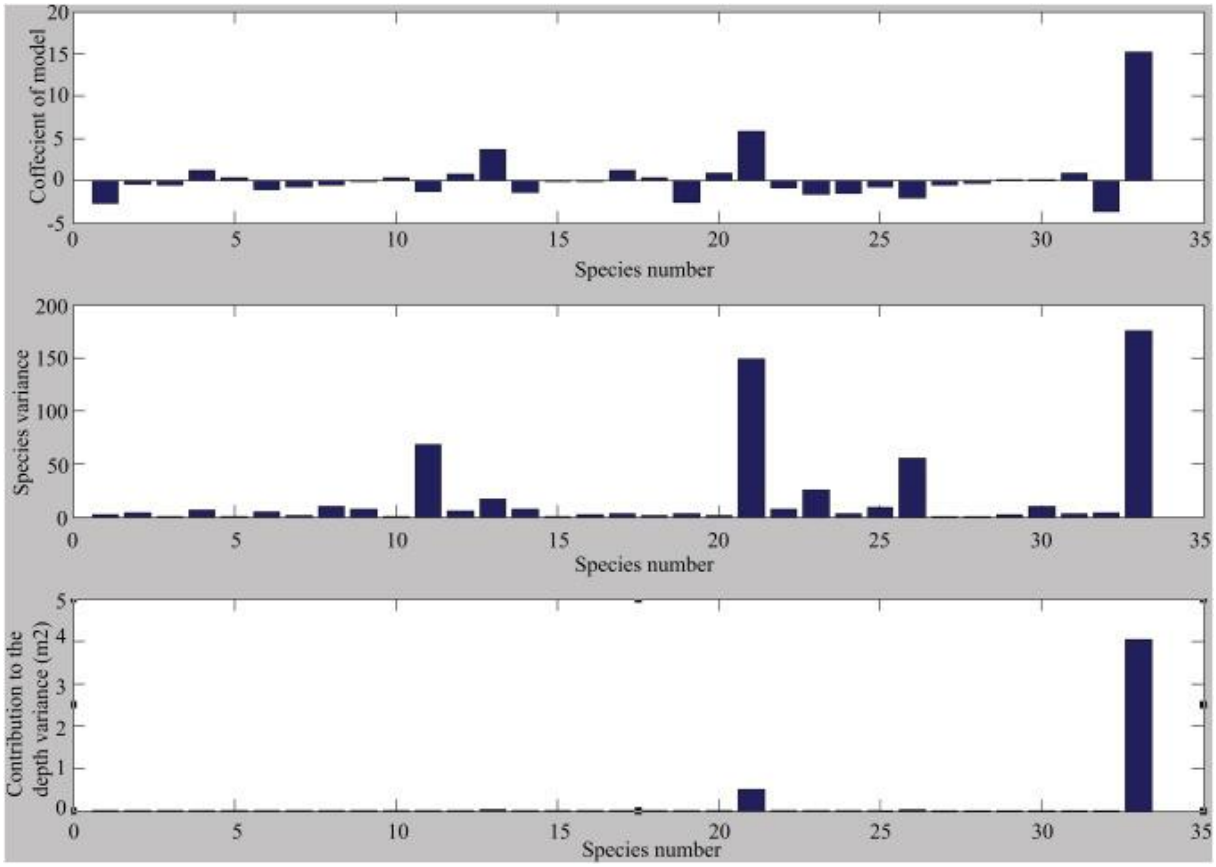

Figure 10: Characterization of the paleo-depth variation during the last 500,000 years. Comparison between: **A:** the relative sea level variation curve (Rohling et al., 2009); **B:** the curve of variation of the modeled paleo-depths; **D** and **E:** curves of changes in oxygen isotopic ratio of benthic (*Cibicides wuellerstofi* and *Cibicides pachyderma*) and planktonic (*Globigerina bulloides*) foraminifers.

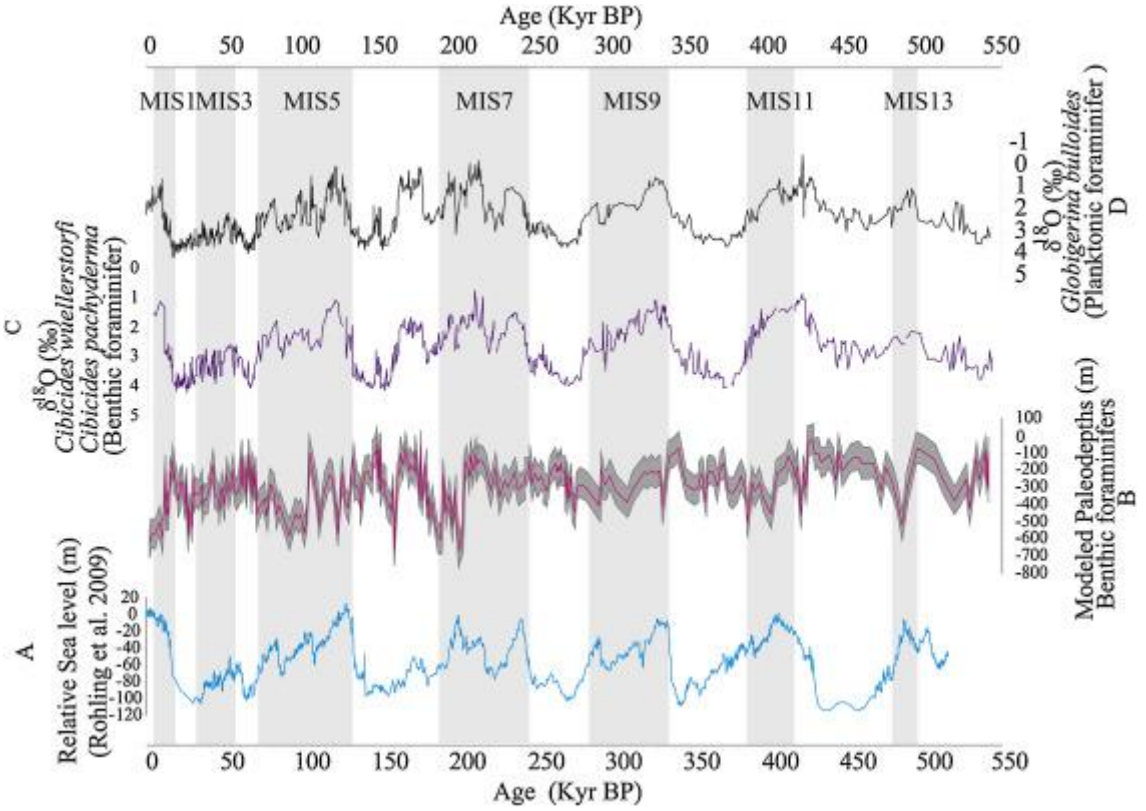

Figure 11: Standardized and smoothed sea level variation curve compared with the smoothed sea level variation curve from Rohling et al. (2009) and the relative abundance variation of benthic foraminifer *Melonis barleeanus* and *Uvigerina mediterranea*. Good correlation is observed between normalized eustatic variations and abundance variations of *Melonis barleeanus* / *Uvigerina mediterranea*. A significant shift during periods of high sea level is observed between the two eustatic curves.

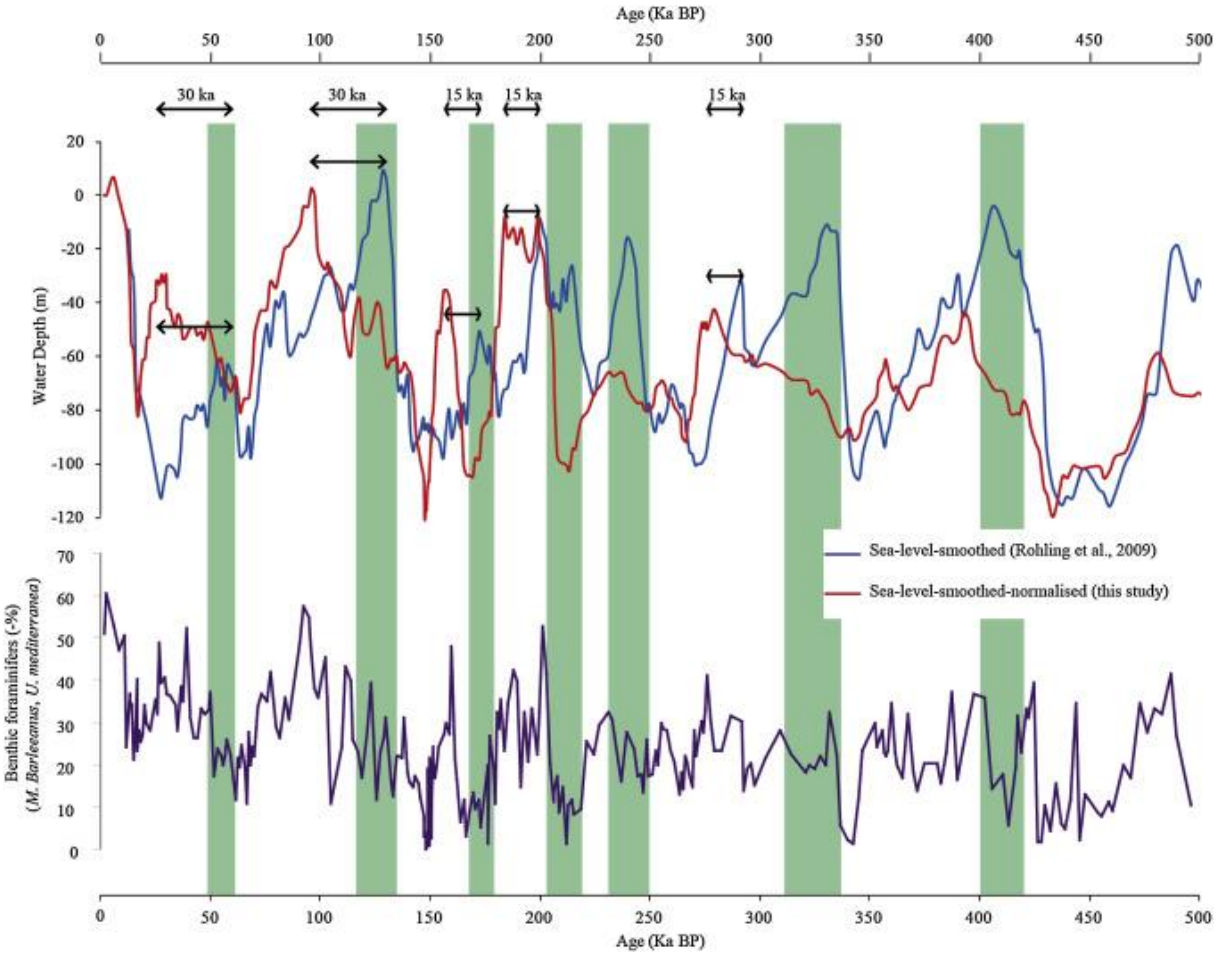

Tables captions

Table 1: Presentation of the 33 benthic foraminifers derived from the analysis of the interface samples and having a median greater than 0. These 33 taxa are selected for the principal component analysis.

Retained species	Order number
Amphicoryna scalaris	1
Bulimina marginata	2
Bulimina costata	3
Bigenerina nodosaria	4
Biloculinella labiata	5
Bolivina spathulata	6
Cibicides wuellerstorfi	7
Cibicides lobatulus	8
Cibicides sp.	9
Cyclogyra carinata	10
Cassidulina carinata	11
Cassidulina crassa	12
Cassidulina minuta	13
Elphidium macelum	14
Fissurina cucullata	15
Gyroidina orbicularis	16
Gyroidina altiformis	17
Hoeglundina elegans	18
Hyalinea balthica	19
Lenticulina sp.	20
Melonis barleeanus	21
Pseudoclavulina crustata	22
Quinqueloculina duthiersi	23
Quinqueloculina viennensis	24
Quinqueloculina seminulum	25
Rosalina globularis	26
Spiroloculina escavata	27
Sigmoilopsis schlumbergeri	28
Spiroplectinella sagitula	29
Textularia agglutinans	30
Textularia truncata	31
Valvulinaria bradyana	32
Uvigerina mediterranea	33